JACS
JOURNAL OF THE AMERICAN CHEMICAL SOCIETY

Communication

pubs.acs.org/JACS

Adding Four Extra K-Regions to Hexa-*peri*-hexabenzocoronene

Tim Dumslaff,[†] Bo Yang,[†] Ali Maghsoumi,[‡] Gangamallaiah Velpula,[§] Kunal S. Mali,[§] Chiara Castiglioni,[§] Steven De Feyter,[§] Matteo Tommasini,[‡] Akimitsu Narita,[†] Xinliang Feng,*[,∥] and Klaus Müllen*[,†]

[†]Max Planck Institute for Polymer Research, Ackermannweg 10, 55128 Mainz, Germany

[‡]Dipartimento di Chimica, Materiali ed Ingegneria Chimica 'G. Natta', Politecnico di Milano, Piazza Leonardo da Vinci 32, 20133 Milano, Italy

[§]Division of Molecular Imaging and Photonics, Department of Chemistry, KU Leuven—University of Leuven, Celestijnenlaan, 200 F, 3001 Leuven, Belgium

[∥]Center for Advancing Electronics Dresden (cfaed) and Department of Chemistry and Food Chemistry, Technische Universität Dresden, Mommsenstrasse 4, 01062 Dresden, Germany

Supporting Information

ABSTRACT: A multistep synthesis of hexa-*peri*-hexabenzocoronene (HBC) with four additional K-regions was developed through a precursor based on two benzotetraphene units bridged with *p*-phenylene, featuring preinstalled zigzag moieties. Characterization by laser desorption/ionization time-of-flight mass spectrometry, Raman and IR spectroscopy, and scanning tunneling microscopy unambiguously validated the successful formation of this novel zigzag edge-rich HBC derivative. STM imaging of its monolayers revealed large-area, defect-free adlayers. The optical properties of the modified HBC were investigated by UV/visible absorption spectroscopy.

Polycyclic aromatic hydrocarbons (PAH) are compounds with multiple fused rings, which are of high interest not only in organic chemistry but also for various applications, including sensing,[1] (opto-)electronics,[2] and catalysis.[3] PAHs that can be drawn with a Kekulé structure without isolated double bonds are called fully benzenoid and are well-known as kinetically very stable and thermodynamically favored substances.[4] Such fully benzenoid PAHs were extensively studied by E. Clar, who assigned their high stability to the localization of aromatic sextets within the molecules.[5] Hexa-*peri*-hexabenzocoronene (HBC) is one of the most important examples of the fully benzenoid PAHs, which can be regarded as "superbenzene" for its extended benzene-like structure with D_{6h}-symmetry.[6] HBCs are marked by their unique optoelectronic behavior, which can be well tuned by chemical modification of its peripheral positions, e.g., with electron-donating or -withdrawing groups.[7]

As opposed to the fully benzenoid compounds, PAHs with K-regions or zigzag periphery show benzenoid structures only in limited areas of the molecules. Such not-fully benzenoid PAHs are typically less stable, but demonstrate interesting properties such as lower band gaps, higher chemical reactivity, and even open-shell biradical character, depending on their structure.[8] The fully benzenoid HBCs can be converted to not-fully benzenoid HBC derivatives with zigzag-edge peripheries by bridging the bay regions with C2 units. In the past, HBCs with one to three extra "double bonds", i.e., K-regions, have thus far been synthesized, demonstrating the varying symmetry and modulated optoelectronic properties.[9] However, HBCs with more than three K-regions have remained elusive.

Herein we present an elegant synthesis and characterizations of a novel HBC derivative with four additional K regions, i.e., "tetrazigzag" HBC (Figure 1). The "tetrazigzag" HBC can also

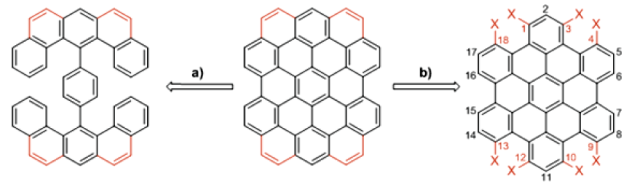

Figure 1. Possible pathways toward HBC with four additional K-regions (red).

be considered as a slightly π-extended analogue of teranthene,[10] but exhibits markedly high stability, enabling its spectroscopic as well as microscopic characterizations under ambient conditions. The structure of the achieved "tetrazigzag"-HBC can thus be unambiguously validated by high-resolution matrix assisted laser desorption/ionization time-of-flight mass spectrometry (MALDI-TOF MS); IR, Raman, and UV/vis absorption spectroscopy with theoretical supports; and scanning tunneling microscopy (STM).

In general, PAHs featured with zigzag edges cannot be simply obtained via planarization of oligophenylene precursors, which poses a challenge for the synthesis of molecules with such structural motifs. To bridge HBC with four additional C2 units one could first think of the possibility to start directly from HBC that is octa-functionalized at the 1, 3, 4, 9, 10, 12, 13, and 18 positions (Figure 1, pathway b). However, such an HBC derivative is not feasible with high regioselectivity by well-established pathways such as cyclotrimerization or Diels–Alder reaction of respective precursors (see Figure S2). Moreover, the formation of four K-regions at the bay positions of HBC would be challenging as well. It is thus more reasonable to design a "double U-shaped" precursor such as the one shown in Figure 1

Received: February 22, 2016
Published: March 23, 2016

DOI: 10.1021/jacs.6b01976
J. Am. Chem. Soc. 2016, 138, 4726–4729

(pathway a), which can directly be cyclized to the target molecule by oxidative cyclodehydrogenation. First attempts using this route were made via conversion of appropriate dibenzo-xanthene precursor **S3** to its pyrylium salt **S4**, followed by nucleophilic oxygen/carbon exchange (see Figure S1). However, this approach failed due to scarce solubility of double-xanthene precursor **S3**, and the introduction of solubilizing chains turned out to be tedious.

Finally, we conceived using a precursor with two phenylene-bridged benzotetraphene units, which serve as preinstalled zigzag edges (molecule **9**, Scheme 1), and elegantly achieved the synthesis of "tetrazigzag" HBC **10**. The key precursor **9** can be prepared through fourfold cycloaromatization of 2,2′′′′-bis((4-(*tert*-butyl)phenyl)ethynyl)-3′,6‴-bis(2-((4-(*tert*-butyl)-phenyl)ethynyl)phenyl)-1,1′:2′,1″:4″,1‴:2‴,1′′′′-quinque-phenyl (**8**), forming the zigzag edges prior to the planarization. To protect the zigzag edges of **10**, additional phenyl rings were introduced, which also enhanced its solubility with the *tert*-butyl groups.

Scheme 1. Synthetic Route towards "tetrazigzag" HBC[a]

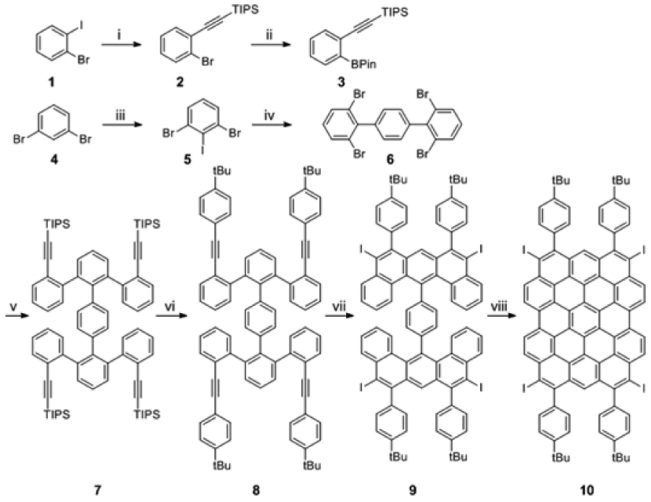

[a]Reagents and conditions: (i) TIPS-acetylene, CuI, $Pd(PPh_3)_2Cl_2$, Et_3N, THF, rt, 9 h, 88%; (ii) *n*-BuLi, THF, −78 °C, isopropyl pinacol borate, 2 h, 73%; (iii) *n*-BuLi, $HN(i\text{-}Pr)_2$, I_2, THF, −78 °C, 2 h, 93%; (iv) 1,4-phenylenebisboronic acid, Pd(dppf), DMSO, H_2O, $NaHCO_3$, 55 °C, 48 h, 31%; (v) **3**, **6**, $Pd(PPh_3)_4$, K_2CO_3, H_2O, dioxane, reflux, 24 h, 78%; (vi) (a) TBAF, DCM, rt, 2 h, (b) 1-*tert*-butyl-4-iodobenzene, piperidine, CuI, $Pd(PPh_3)_4$, 60 °C, 4 h, 80%; (vii) bis(pyridine)iodonium-tetrafluoroborate, TFMSA, DCM, −40 °C, 6 h, 58%; (viii) DDQ, TFMSA, DCM, rt, 16 h, 87%. DCM: dichloro-methane. TFMSA: trifluoromethanesulfonic acid.

Toward the synthesis of precursor **9**, triisopropyl((2-(4,4,5,5-tetramethyl-1,3,2-dioxaborolan-2-yl)phenyl)-ethynyl)silane (**3**) was first prepared by selective Sonogashira−Hagihara coupling of 1-iodo-2-bromobenzene **1** with tri(isopropyl)silyl (TIPS)-acetylene, followed by a borylation reaction, using *n*-BuLi and 2-isopropoxy-4,4,5,5-tetramethyl-1,3,2-dioxaborolane. On the other hand, 2,2″,6,6″-tetrabromo-1,1′:4′,1″-terphenyl **6** was obtained through iodination of 1,3-dibromobenzene **4** with lithium diisopropylamide (LDA)/iodine followed by Suzuki coupling with 1,4-phenylenebisboronic acid. Boronic ester **3** and tetrabromoterphenyl **6** were subjected to a Suzuki coupling to form **7** in 78% yield. Deprotection of the ethynyl groups with tetrabutylammonium fluoride (TBAF) and subsequent fourfold Sonogashira−Hagihara coupling with 1-*tert*-butyl-4-iodoben-zene gave compound **8** in 80% yield over two steps.

For the key ring forming step from **8** to **9**, trifluoroacetic acid was first tested as the electrophilic reagent,[11] but it was not possible to achieve the fourfold cyclization, only providing a complex mixture of partially fused products. Nevertheless, the fourfold cyclization of **8** could be completed by employing a stronger electrophile, iodonium tetrafluoroborate, which was generated in situ at low temperatures, following the procedure reported by Goldfinger et al.[12] Precursor **9** could thus be obtained in 58% yield and unambiguously characterized by the single-crystal X-ray and ^1H NMR analyses (Figure 2). The single-crystal structure of **9** (Figure 2a) confirmed the distortion of this molecule which adopts a C_i-symmetric conformation. The two highly twisted benzotetraphene units are herein independent from each other due to the flexible phenylene spacer in between. The ^1H NMR shows clearly resolved signals (Figure 2b), which could be fully assigned using the H−H COSY method (see Supporting Information (SI)).

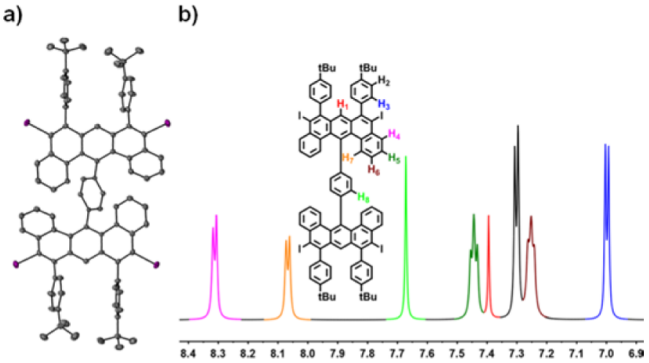

Figure 2. (a) View of molecular structure determined by single-crystal X-ray crystallography of **9**. (b) Aromatic region of the ^1H NMR spectrum of **9**, recorded in 1,1,2,2-tetrachloroethane-d_2 at 100 °C (700 MHz).

Finally, precursor **9** was planarized through the oxidative cyclodehydrogenation using 2,3-dichloro-5,6-dicyano-1,4-benzoquinone (DDQ)/trifluoromethane-sulfonic acid (TFSA), to afford "tetrazigzag" HBC **10** in 87% yield as a dark purple solid. Attempts to remove the four iodo groups coincided with oxidation, indicating that these halogens attached to the zigzag peripheries indeed stabilized the molecule.

Because of the strong aggregation in solution even at a dilution of 5×10^{-5} mol/L, the structure of **10** could not be analyzed by NMR spectroscopy and single-crystal X-ray analysis.[13] NMR measurements at temperatures up to 140 °C and with CS_2 as an additive to destroy aggregation did not improve the spectral resolution. The possible radical character of the molecule was also excluded by adding hydrazine as radical quencher and measuring NMR at lower temperatures down to −120 °C, resulting in a spectrum consisting of unresolved signals.

Nevertheless, characterizations by combination of MALDI-TOF MS, IR, and Raman spectroscopy as well as STM analysis clearly validated the formation of "tetrazigzag" HBC **10**. Figure 3a shows the MALDI-TOF MS spectrum of **10**, which displays an intense signal at m/z = 1650.1038 in perfect agreement with its expected molecular mass of 1650.1030. The signal with

DOI: 10.1021/jacs.6b01976
J. Am. Chem. Soc. 2016, 138, 4726−4729

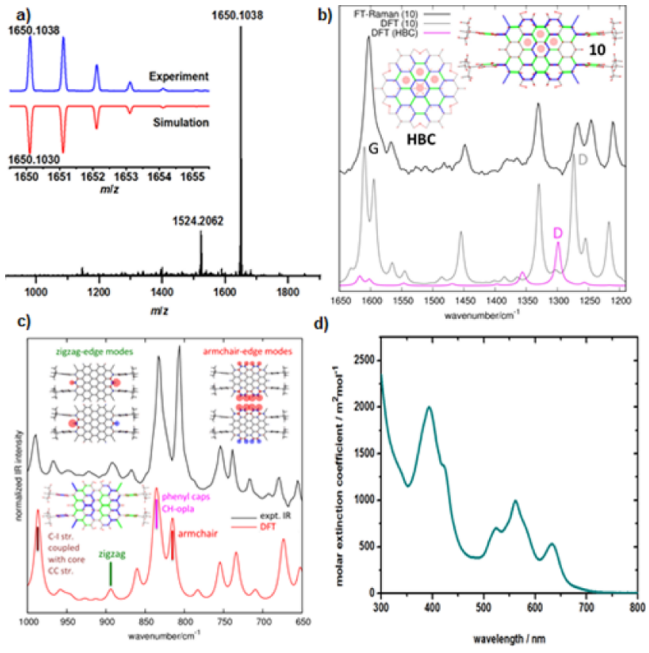

Figure 3. (a) MALDI-TOF MS spectrum of tetrazigzag HBC **10**. Inset: isotopic distribution compared with mass spectrum simulated for $C_{90}H_{62}I_4$. (b) FT-Raman (1064 nm) spectrum of **10** compared with results from DFT calculations over the D and G regions. DFT-calculated spectrum of the parent HBC is also displayed for comparison. (c) Micro IR spectrum of **10**. Inset: out-of-plane modes. The size of blue/red circles of the molecular sketch is proportional to nuclear displacements in the out-of-plane direction (z); red indicates displacements directed along $+z$, and blue indicates displacements directed along $-z$. (d) UV/vis absorption spectrum of **10** in THF.

lower intensity appearing at m/z = 1524.2062 corresponds to the loss of one iodine atom, which is caused by the high laser power necessary to ionize this large PAH molecule. Furthermore, the observed isotopic distribution was fully consistent with the simulated spectrum (red line) based on the elemental composition of $C_{90}H_{62}I_4$, further corroborating the formation of "tetrazigzag" HBC **10**.

The FT-Raman analysis was performed on a powder sample of "tetrazigzag" HBC **10** with excitation at 1064 nm (Figure 3b). The experimental FT-Raman spectrum is in accordance with the DFT-calculated spectrum, which offers further evidence for the successful formation of **10**. The nuclear displacements associated with the D-peak found for **10** compare with the displacement pattern found in the parent HBC. Resulting from a larger π-conjugation, the D-peak of **10** is red-shifted and shows higher Raman activity, compared to that of the parent HBC (Figure 3b).

Next, the IR spectrum of a powder sample of **10** was measured in a diamond anvil cell and compared with a DFT-calculated spectrum (Figure 3c). Significantly, the experimental IR spectrum is in full agreement with the calculated IR signals. It is remarkable to note that the armchair-edge modes can be found at 807 cm^{-1} (832 cm^{-1}, unscaled DFT), while a low intensity band at 892 cm^{-1} (912 cm^{-1}, unscaled DFT) can be assigned to the characteristic zigzag-edge modes. The aryl groups that stabilize the zigzag edges show a C−H out-of-plane bending at 832 cm^{-1} (853 cm^{-1}, unscaled DFT) while the additional iodine atoms cause a medium IR absorption band at 990 cm^{-1} (1007 cm^{-1}, unscaled DFT).

DFT calculations on "tetrazigzag" HBC **10** manifested its highest occupied molecular orbital (HOMO) and lowest unoccupied molecular orbital (LUMO) levels at −4.97 and −2.47 eV, respectively, with a HOMO−LUMO gap of 2.50 eV. As expected for the extended aromatic system, this value is the smallest among the reported "zigzag" HBC series, being 1.1 eV lower than that of the parent HBC and 0.3 eV smaller compared to the "dizigzag" HBC with the same D_{2h} symmetry.[9b] For comparison, the aromatic core structure of **10** substituted with H (**10H**; see Figure 1) was also calculated, showing its HOMO at −4.76 eV and LUMO at −2.25 eV with a HOMO−LUMO gap of 2.51 eV, exhibiting slight deviation of the energy levels compared to those of **10**.

Furthermore, the optical properties of **10** were studied by UV/vis absorption spectroscopy as well as the time-dependent density functional theory (TDDFT) calculations (Figure 3d and Table S1). A solution of **10** in THF showed no change in the UV/vis spectrum over two months at room temperature under air, marking the high stability of **10**. The TDDFT calculations on **10** unveiled three optically allowed vertical transitions with large oscillator strengths at 547 nm (2.27 eV, p-band), 405 nm (3.06 eV, β-band), and 378 nm (3.28 eV, β'-band), which fairly match the observed absorption peaks at 562 nm (2.21 eV), 421 nm (2.95 eV), and 394 nm (3.15 eV), respectively. Here, p-, β-, and β'-bands are based on Clar's notation and mainly correspond to HOMO → LUMO, HOMO → LUMO+1, and HOMO−1 → LUMO+1 transitions, respectively.[5,9b,14] The α-band, which is normally expected for PAHs, cannot be found in the recorded UV/vis spectrum due to the strong p-band that is split into three signals by the vibronic coupling (Figure 3d). TDDFT calculations on unsubstituted "tetrazigzag" HBC **10H** shows its optical transitions at similar energies to those of **10**, pointing to the limited effect of the substituents (see Table S1 in SI). Compared to the parent HBC and the D_{2h} symmetrical "dizigzag" HBC, the calculated p-band of **10H** is red-shifted by 128 nm (0.72 eV) and 64 nm (0.31 eV), respectively,[9b] which is in line with the trend observed for the HOMO−LUMO gaps.

The self-assembly behavior of **10** was studied by characterizing its monolayer formed at the 1,2,4-trichlorobenzene (TCB)/highly oriented pyrolytic graphite (HOPG) interface using STM. "Tetrazigzag" HBC **10** assembles to form a highly ordered defect-free monolayer that extends several hundred square nanometers (Figure S4). The strong solution aggregation tendency of **10** is also reflected in the monolayer, where molecules show different apparent heights in STM images, which is reminiscent of stacked structures (see SI).

The monolayer of **10** shows rectangular bright features organized in a brick-wall type structure, where each bright rectangle represents a single molecule of **10** (Figure 4a). Close inspection of the STM image reveals that unit cell vector 'a' is shorter than vector 'b'. A molecular model based on unit cell parameters (Figure 4b) indicates that iodine−iodine interactions possibly contribute to the stabilization of the monolayer along the 'a' vector of the unit cell. The spacing of molecular rows along the other unit cell vector is determined by the *tert*-butyl groups. Each molecule appears as a group of four protrusions (inset Figure 4a), which tentatively correspond to the location of *tert*-butyl groups. It has been well documented that molecular orbitals corresponding to the *tert*-butyl groups dominate the contrast in STM images of aromatic molecules substituted with *tert*-butyl.[15]

DOI: 10.1021/jacs.6b01976
J. Am. Chem. Soc. 2016, 138, 4726−4729

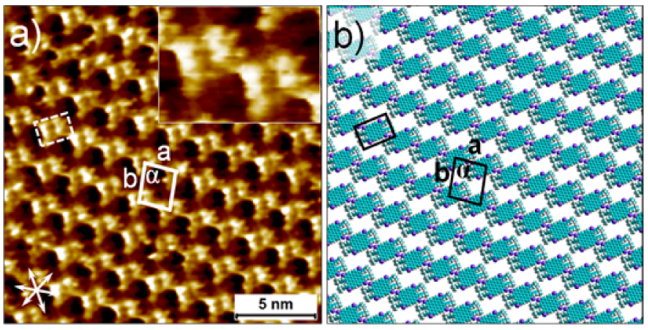

Figure 4. (a) STM image of a self-assembled monolayer of **10**. Unit cell is overlaid on the image and the cell parameters are $a = 2.0 \pm 0.1$ nm, $b = 2.5 \pm 0.1$ nm, and $\alpha = 78 \pm 2.0°$ (one molecule per unit cell). The inset shows a digital zoom of the image showing submolecular features. Tunneling current, $I_{set} = 120$ pA, Sample bias, $V_{bias} = -550$ mV. (b) Molecular model of the self-assembled network of **10**.

In summary, we achieved the synthesis of a new stable not-fully benzenoid HBC derivative with four additional K-regions, based on a precursor with two prefused benzotetraphene units. Notably, experimental IR and Raman spectra display remarkable agreement with theoretical ones, elucidating specific peaks originating from the armchair and zigzag peripheries. UV/vis absorption analysis and theoretical studies of **10** demonstrated a significant red shift of the absorption and lowering of the HOMO−LUMO gap compared to the parent HBC and its derivatives with one to three K-regions. The DFT calculation on **10** revealed its lowered HOMO−LUMO gap of 2.50 eV, which makes **10** an interesting candidate for the optoelectronic applications such as in photovoltaic cells. The synthetic design of **10** offers the opportunity for further functionalization utilizing the four peripheral iodo groups as well as the two remaining bay regions. Especially, addition of C2 units to the remaining bay regions can lead to the long awaited "circumcoronene" that is fully surrounded by the zigzag edges.

■ ASSOCIATED CONTENT

Supporting Information

The Supporting Information is available free of charge on the ACS Publications website at DOI: 10.1021/jacs.6b01976.

Experimental details, NMR, MALDI-TOF MS, UV/vis absorption spectra (PDF)
Crystallographic data (CIF)

■ AUTHOR INFORMATION

Corresponding Authors

*xinliang.feng@tu-dresden.de
*muellen@mpip-mainz.mpg.de

Notes

The authors declare no competing financial interest.

■ ACKNOWLEDGMENTS

We are grateful for the financial support from the European Research Council grant on NANOGRAPH and NANOGRAPH@LSI (No. 340324), DFG Priority Program SPP 1459, Graphene Flagship (No. CNECT-ICT-604391), and European Community through the FET-Proactive Project "MoQuaS" (No. 610449) and Marie-Curie projects ITN iSwitch (GA No. 642196). S.D.F., K.M., and G.M. thank the Fund of Scientific Research−Flanders (FWO), KU Leuven (GOA 11/003), and Belgian Federal Science Policy Office (IAP-7/05).

■ REFERENCES

(1) (a) Liu, J.; Liu, Z.; Barrow, C. J.; Yang, W. *Anal. Chim. Acta* **2015**, *859*, 1. (b) Bachar, N.; Liberman, L.; Muallem, F.; Feng, X.; Muellen, K.; Haick, H. *ACS Appl. Mater. Interfaces* **2013**, *5*, 11641.
(2) (a) Ponomarenko, L. A.; Schedin, F.; Katsnelson, M. I.; Yang, R.; Hill, E. W.; Novoselov, K. S.; Geim, A. K. *Science* **2008**, *320*, 356. (b) Wu, J.; Pisula, W.; Muellen, K. *Chem. Rev.* **2007**, *107*, 718.
(3) Machado, B. F.; Serp, P. *Catal. Sci. Technol.* **2012**, *2*, 54.
(4) Clar, E. *The aromatic sextet*; J. Wiley: London, 1972.
(5) Clar, E. *Polycyclic Hydrocarbons*; Academic Press: New York, 1964.
(6) Ito, S.; Herwig, P. T.; Bohme, T.; Rabe, J. P.; Rettig, W.; Muellen, K. *J. Am. Chem. Soc.* **2000**, *122*, 7698.
(7) (a) Yamaguchi, R.; Ito, S.; Lee, B. S.; Hiroto, S.; Kim, D.; Shinokubo, H. *Chem. - Asian J.* **2013**, *8*, 178. (b) Wong, W. W. H.; Subbiah, J.; Puniredd, S. R.; Purushothaman, B.; Pisula, W.; Kirby, N.; Muellen, K.; Jones, D. J.; Holmes, A. B. *J. Mater. Chem.* **2012**, *22*, 21131. (c) Jones, D. J.; Purushothaman, B.; Ji, S.; Holmes, A. B.; Wong, W. W. H. *Chem. Commun.* **2012**, *48*, 8066. (d) Tan, Y.-Z.; Osella, S.; Liu, Y.; Yang, B.; Beljonne, D.; Feng, X.; Muellen, K. *Angew. Chem., Int. Ed.* **2015**, *54*, 2927. (e) Doessel, L. F.; Kamm, V.; Howard, I. A.; Laquai, F.; Pisula, W.; Feng, X.; Li, C.; Takase, M.; Kudernac, T.; De Feyter, S.; Muellen, K. *J. Am. Chem. Soc.* **2012**, *134*, 5876.
(8) (a) Wassmann, T.; Seitsonen, A. P.; Saitta, A. M.; Lazzeri, M.; Mauri, F. *J. Am. Chem. Soc.* **2010**, *132*, 3440. (b) Sun, Z.; Zeng, Z.; Wu, J. *Chem. - Asian J.* **2013**, *8*, 2894. (c) Sun, Z.; Ye, Q.; Chi, C.; Wu, J. *Chem. Soc. Rev.* **2012**, *41*, 7857. (d) Kubo, T. *Chem. Rec.* **2015**, *15*, 218. (e) Kubo, T. *Chem. Lett.* **2015**, *44*, 111.
(9) (a) Feng, X.; Wu, J.; Ai, M.; Pisula, W.; Zhi, L.; Rabe, J. P.; Muellen, K. *Angew. Chem., Int. Ed.* **2007**, *46*, 3033. (b) Kastler, M.; Schmidt, J.; Pisula, W.; Sebastiani, D.; Muellen, K. *J. Am. Chem. Soc.* **2006**, *128*, 9526. (c) Wang, Z. H.; Tomovic, E.; Kastler, M.; Pretsch, R.; Negri, F.; Enkelmann, V.; Muellen, K. *J. Am. Chem. Soc.* **2004**, *126*, 7794.
(10) Konishi, A.; Hirao, Y.; Nakano, M.; Shimizu, A.; Botek, E.; Champagne, B.; Shiomi, D.; Sato, K.; Takui, T.; Matsumoto, K.; Kurata, H.; Kubo, T. *J. Am. Chem. Soc.* **2010**, *132*, 11021.
(11) Goldfinger, M. B.; Crawford, K. B.; Swager, T. M. *J. Org. Chem.* **1998**, *63*, 1676.
(12) Goldfinger, M. B.; Crawford, K. B.; Swager, T. M. *J. Am. Chem. Soc.* **1997**, *119*, 4578.
(13) (a) Kastler, M.; Pisula, W.; Wasserfallen, D.; Pakula, T.; Muellen, K. *J. Am. Chem. Soc.* **2005**, *127*, 4286. (b) Wasserfallen, D.; Kastler, M.; Pisula, W.; Hofer, W. A.; Fogel, Y.; Wang, Z. H.; Muellen, K. *J. Am. Chem. Soc.* **2006**, *128*, 1334.
(14) Rieger, R.; Muellen, K. *J. Phys. Org. Chem.* **2010**, *23*, 315.
(15) Jung, T. A.; Schlittler, R. R.; Gimzewski, J. K. *Nature* **1997**, *386*, 696.

DOI: 10.1021/jacs.6b01976
J. Am. Chem. Soc. 2016, 138, 4726−4729